research article

Relation of the chondromalatia patellae to proximal tibial anatomical parameters, assessed with MRI

Mohammadreza Tabary[1], Azadehsadat Esfahani[2], Mehdi Nouraie[3], Mohammad Reza Babaei[4], Ali Reza Khoshdel[5], Farnaz Araghi[6], Mostafa Shahrezaee[1,7]

[1] Department of Science and Research Branch, AJA University of Medical Sciences, Tehran, Iran
[2] School of Medicine, Tehran University of Medical Sciences, Tehran, Iran
[3] Division of Pulmonary, Allergy and Critical Care Medicine, Department of Medicine, University of Pittsburgh, Pittsburgh, PA, USA
[4] Department of Interventional Radiology, Firouzgar Hospital, Iran University of Medical Sciences, Tehran, Iran
[5] Modern Epidemiology Research Center, AJA University of Medical Sciences, Tehran, Iran
[6] School of Medicine, Shahid Beheshti University of Medical Sciences, Tehran, Iran
[7] Department of Orthopedics, AJA University of Medical Sciences, Tehran, Iran

Radiol Oncol 2020; 54(2): 159-167.

Received 13 February 2020
Accepted 18 March 2020

Correspondence to: Mostafa Shahrezaee, M.D., Professor of Orthopedics, Department of Science and Research Branch, AJA University of Medical Sciences, Etemadzadeh St., Tehran, Iran. E-mail: moshahrezayee@yahoo.com

Disclosure: No potential conflicts of interest were disclosed.

Background. Magnetic resonance imaging (MRI) is a non-invasive highly sensitive tool for diagnosing chondromalacia patellae in the early stages. Many studies have evaluated patellar and trochlear morphology with different radiologic indices. We aimed to assess the discriminative power of tibial, patellar, and femoral indices in MRI for chondromalacia patellae.

Patients and methods. 100 cases of chondromalacia, as well as 100 age-matched controls among the patients who underwent knee MRI between February 2017 and March 2019, were included. The standard protocol of knee MRI was applied and the diagnosis of chondromalacia was made on MRI findings. Chondromalacia subjects were also classified as grade 1 to 4 according to the Modified Outerbridge's MRI grading system. We measured 25 MRI parameters in the knee and adjacent structures to determine the relation between chondromalacia patellae and anatomical MRI parameters.

Results. Tibial slope, trochlear depth, lateral trochlear inclination, and lateral patellar tilt angle had significant correlation with chondromalacia. Any increase in lateral trochlear inclination and lateral patellar tilt angle could increase the probability of the disease (Odds ratio [OR] 1.15, 1.13; 95% CI: 1.03–1.30; 1.02–1.26, respectively), while any increase in medial tibial slope and trochlear depth could decrease the probability of chondromalacia (OR 0.85, 0.06; 95% CI: 0.73–0.98, 0.02–0.17, respectively). We also designed a model for the severity of disease by using the patellar height index (relative odds ratio: 75.9).

Conclusions. The result of this study showed the novelty role of tibial anatomy in developing chondromalacia and its mechanism. We also concluded that patellar height might be an important factor in defining disease severity.

Key words: magnetic resonance imaging; chondromalacia patellae; anatomical indices

Introduction

Chondromalacia patellae is a common reason for patellofemoral pain syndrome. It is defined as the disruption of patellar cartilage due to repeated stress to the articular surface.[1] These patients may experience frequent recurrence and chronic pain, which limits daily life activities.[2] Radiographs

were traditionally used to diagnose chondromalacia; however, this modality was unable to visualize patellar alignment and congruency angles[3], and the complete anatomy was not visualized using X-ray.

Magnetic resonance imaging (MRI), a non-invasive tool to detect chondromalacia patellae with a high soft tissue contrast, can detect chondromalacia in the lower stages with a sensitivity of 66%. Moreover, this sensitivity rises to 85–100% for the higher stages.[4] Many key findings can be detected in the early stage of chondral loss including signal irregularities, fissures, and chondral thinning; thus, leading to earlier diagnosis.[5]

Multiple mechanisms can cause chondromalacia, including vascular insufficiency, trauma, and structural abnormalities.[6] In line with the mechanism of structural abnormalities, many studies have evaluated patellar and femoral trochlear morphology with different radiologic indices. Femoral intertrochlear notch angle, femoral trochlear depth, femoral sulcus angle, femoral trochlear angle, patellar tilt angle, and patellar height indices were among these factors. Many patellar height indices, measured as patellar tendon to patellar length ratio, seemed to correlate with cartilage defects.[7] Furthermore, the correlation between tibial structural abnormalities and patellar cartilage stress, but not cartilage defects, was evaluated previously.[8] On the other hand, some studies focused on the correlation between soft tissue structure and chondromalacia, particularly subcutaneous fat and adjacent muscles.[8, 9]

Radiologic findings of the knee joint differ between low-grade (grade 1, 2) and high-grade (grade 3,4) chondromalacia. For instance, the sulcus angle and trochlear depth were shown to be significantly different between mild and severe cartilage defects.[10]

The role of tibial anatomy is not well-known in developing chondromalacia. Some studies evaluated the role of tibial anatomy in dynamic models, but not in human subjects.[11]

To our knowledge, there is no published diagnostic model of radiological findings for chondromalacia that includes all important findings including tibial anatomical parameters. We aimed to develop a model and assess the discriminative power of tibial, patellar, and femoral indices for chondromalacia and emphasize the role of tibial anatomy for the first time. We also hypothesize that patellar height is a substantial factor, affecting the development of the disease.

Patients and methods

Patients and population

We reviewed all the radiology records of the patients who underwent knee MRI in our institute between February 2017 and March 2019. We reviewed almost 2000 MRI images of the patients who referred to our institution. After reviewing all the images, we included 200 cases of chondromalacia patellae without any other accompanied diseases in MRI images. The diagnosis of chondromalacia was made on MRI findings including irregularity of the cartilage and the loss of cartilage thickness in at least two consecutive slices. The exclusion criteria were as follows: age more than 65 or less than 18, history of trauma to the knee and adjacent structures in the last 6 months, history of knee surgery, osteoarthritis grade 3 and 4, presence of a fracture or space-occupying lesion in MRI, and patellar subluxation. Patients were contacted and referred to our clinic for clinical evaluation. Patients with other clinical signs not related to chondromalacia were also excluded. After applying exclusion criteria and considering clinical signs, we included 100 cases of chondromalacia patellae. Chondromalacia cases were also classified as grade 1 to 4 according to the Modified Outerbridge's MRI grading system.[12] In case of the presence of more than a single grade lesion, the higher grade was selected.

After reviewing MRI images, we selected 200 controls without any significant changes in bony, ligamentous, chondral, tendinous, and muscular structures around the knee. Selection bias was minimized by using case-matched controls regarding age, gender, and BMI. The patellar cartilage was evaluated intact in the control group. After clinical evaluation, we excluded 100 controls with positive clinical finding in the knee. We finally included 100 healthy matched controls in the final analysis. A radiologist experienced in musculoskeletal imaging (A.E.) performed all the measurements. The same radiologist repeated the MRI measurement after 4 weeks in a random sample of the whole population to test the intra-rater reliability. The reader was blinded to participant's names, sex, age. The ethical approval for this study was obtained from local ethics committee and written consent was obtained from the patients.

MRI evaluation

A 1.5 Tesla Achieva (Philips, Best, Netherlands) MRI device with an extremity superficial coil was used to perform the scans. All the measurements

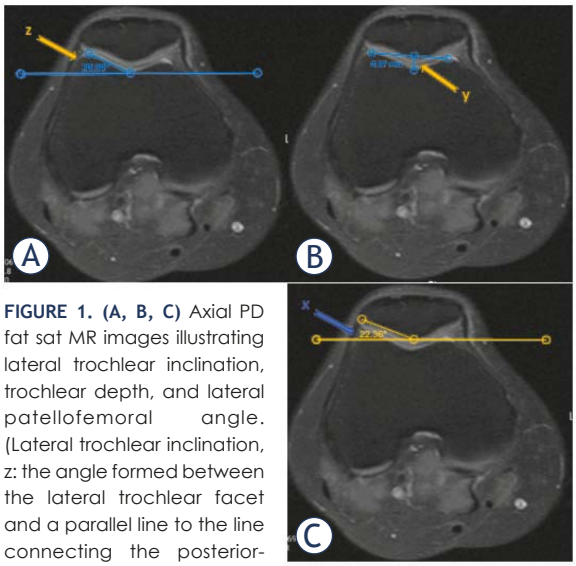

FIGURE 1. (A, B, C) Axial PD fat sat MR images illustrating lateral trochlear inclination, trochlear depth, and lateral patellofemoral angle. (Lateral trochlear inclination, z: the angle formed between the lateral trochlear facet and a parallel line to the line connecting the posterior-most cortical surfaces of the femoral condyles; Trochlear depth, y: the distance between the deepest point of trochlear sulcus and the line connecting the anterior points of the medial and lateral condyles; Lateral patellar tilt angle, x: the angle between the line parallel to the patellar lateral facet and the line connecting the most posterior parts of femoral condyles)

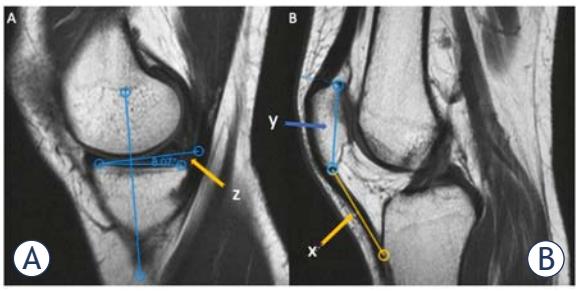

FIGURE 2. (A, B) Sagittal T1-Weighted MR images illustrating medial tibial slope and Insall-Salvati index. (Medial tibial slope, z: the angle formed between the line running along the tibial slope of the medial tibial condyle and the perpendicular line to the tibial axis; Insall-Salvati index: the ratio of x to y; x, the length of patellar tendon and y, the greatest diagonal length of patella)

and processing were performed in the Picture Archiving Communication System (Marco PACS, Version 10). The standard protocol of knee MRI was applied (neutral knee position) with a slice thickness of 3 mm. T1 and T2 (sagittal), Proton density (PD) fat saturation (axial, coronal, and sagittal) sequences were recorded. We measured 25 MRI parameters in the knee and adjacent structures. The definition and the procedure of all measurements were described elsewhere and are summarized in Figure 1,2,3 (Figure 1 & Figure 2 illustrates the significant MRI measurements in the final model). Intercondylar notch angle (INA), medial tibial slope (MTS), lateral tibial slope (LTS), anterior tibial slope (ATS), coronal tibial slope (CTS), intercondylar depth (ID), condylar width (CW), intercondylar width (IW), medial condylar width (MCW), lateral condylar width (LCW), notch width index (NWI), and patellar tendon tibial shaft (PTTS) angle were evaluated in previous studies in cruciate ligament injuries[13-15], but not in chondromalacia subjects. Subchondral and cartilaginous Wiberg-angle (SWA and CWA) were evaluated in trochlear dysplasia[16], but not in chondromalacia patients. Tilting deformity was evaluated in healthy subject by using patellar-patellar tendon (P-PT) angle[17]; however, it was not evaluated in chondromalacia cases. Lateral patellar tilt angle (LPTA), sulcus angle (SA), trochlear depth (TD), lateral trochlear inclination (LTI), medial trochlear inclination (MTI), patellar facet angle (PFA) and trochlear angle (TA) were studied in chondromalacia cases; however, the controls were not matched to the cases regarding gender and BMI.[18] Also, they were analyzed in a single variable model using *student t-test* method and not in a multi-variable model. Tibial tuberosity-trochlear groove (TTTG) distance was described in patellofemoral pain syndrome[19], but not assessed specifically in chondromalacia cases. Patellar height index was also described in previous studies[20]; however, we evaluated the predictive power of Insall-Salvati index (ISI) for the severity (grading) of the disease.

Statistical analysis

MRI measurements were presented in the case and control group by median (interquartile range). Odds ratio (95% CI) for each measurement was calculated including the clustering of observations within subjects. We applied multiple alternative variable selection approaches, including backward and forward stepwise approach to develop the most parsimonious predictive model with the highest calibration. Final model was selected based on Akaike Information Criterion. Then we applied bootstrapping (with 50 replications) to assess the internal validity of the model. The final Odds ratio (95%CI) was reported from bootstrapping results. In the final model, we calculated the Area Under Curve using bootstrapping internal validation. Same analysis approach was replicated to compare two group of cases with low disease severity (grade 1, 2) vs. high severity (grade 3,4). Intra-class correlation coefficient was used to assess intra-rater reli-

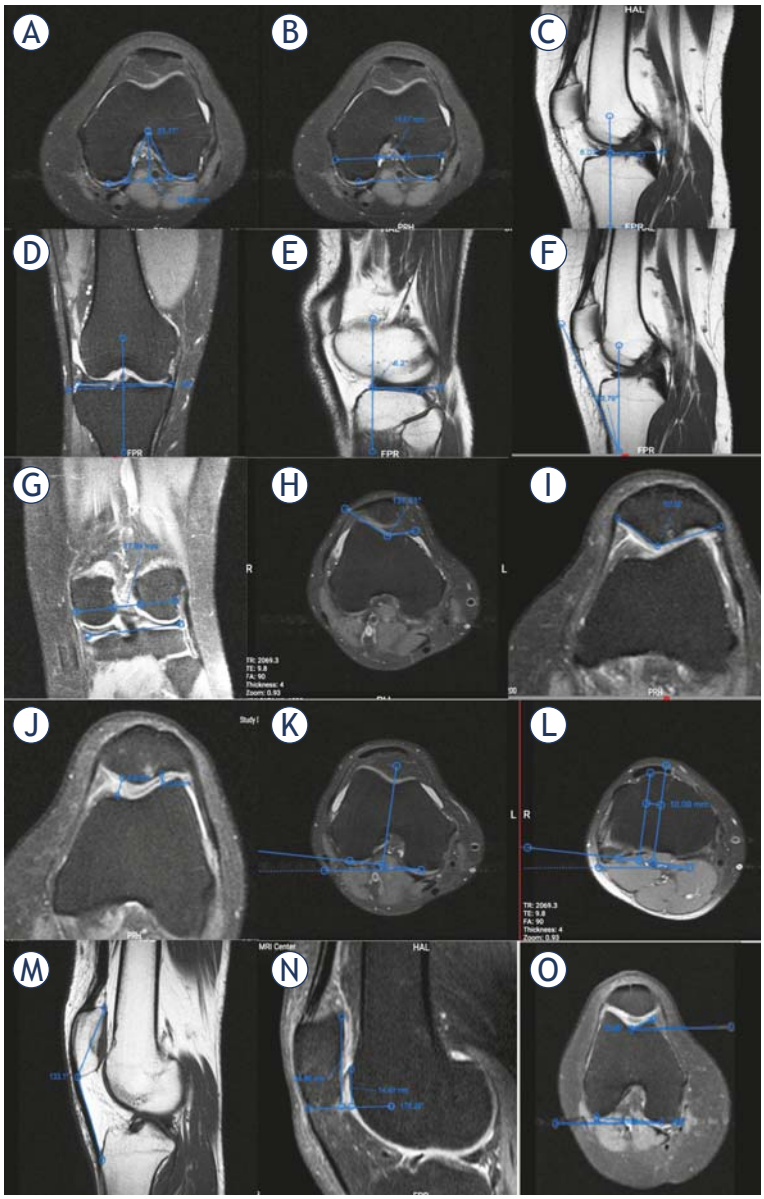

FIGURE 3. Measurements of nonsignificant MRI parameters in the final model. **(A)** Axial MRI plane of the knee showing Intercondylar notch angle (INA) and Intercondylar depth (ID): The posterior bicondylar line is drawn. ID is the distance between top of the notch to the bi-epicondylar line. Intercondylar notch angle is defined as the angle formed by the 2 lines going from the top of the notch to the most inferior aspect of the notch at the medial and lateral condyles; **(B)** Axial MRI plane of the knee showing Intercondylar Width (IW), Medial condyle width (MCW), and Lateral condyle width (LCW): IW is the distance between the medial and lateral femoral condyle walls at the anterior third of the intercondylar depth (the middle line), the other two distances in this axial cut represent LCW, and MCW; **(C)** Sagittal MRI plane of the knee showing anterior tibial slope (ATS): At first the tibial axis is drawn by joining to midpoints between the anterior and posterior cortex of the tibial diaphysis with at least 5cm distance from each other. The anterior tibial slope is then defined as the angle between a perpendicular line (inferior line) to the longitudinal axis and a line passing through the anterior cruciate ligament tibial footprint (superior line); **(D)** Sagittal MRI plane of the knee showing coronal tibial slope (CTS): The coronal tibial slope is defined as the angle between a line joining the highest points on the medial and lateral aspects of the tibial plateau (inferior horizontal line) and a perpendicular line (superior horizontal white line) to the longitudinal axis as mentioned above; **(E)** Sagittal MRI plane of the knee showing lateral tibial slope (LTS): the angle formed between the line running along the tibial slope of the medial tibial condyle and the perpendicular line to the tibial axis; **(F)** Sagittal MRI plane of the knee showing patellar tibial tendon shaft angle (PTTS angle): PTTS angle is measured as the angle between Proximal tibial anatomical axis described above and patellar tendon axis in the mid-sagittal section; **(G)** Coronal MRI plane of the knee showing notch width index (NWI): first Bicondylar width parallel to the joint line at the level of popliteal groove is measured (1). Then notch width is measured at the level of popliteal groove, using the line joining the innermost margins of the femoral condyles at the borders of the intercondylar notch (2). The NWI is ratio of 2/1; **(H)** Axial MRI plane of the knee showing sulcus angle (SA): The angle formed between the medial and lateral trochlear facets; **(I)** Axial MRI plane of the knee showing patellar facet angle (PFA): the angle between two line connecting the central ridge to the middle of patellar facets; **(J)** Axial MRI plane of the knee showing patellofemoral index (PFI): the ratio of medial to lateral interspaces; **(K, L)** Axial MRI plane of the knee showing tibial tuberosity trochlear groove distance (TTTG): posterior line was drawn at posterior border of femoral condyles. A vertical line is drawn at trochlear groove and the other parallel line is drawn along the tibial tuberosity that transferred to this level. Distance between the two lines is measured as TT-TG; **(M)** Sagittal MRI plane of the knee showing Patella-patellar tendon angle (P-PT angle): The P–PT angle was defined as the angle between the upper patellar pole and the lower patellar pole, and the tibial tuberosity; **(N)** Sagittal MRI plane of the knee showing Patellotrochlear index (PTI): it is defined as the length of patellar cartilage overlapping the trochlear cartilage divided by length of patellar cartilage; **(O)** Axial MRI plane of the knee showing medial trochlear inclination (MTI): the angle formed between the medial trochlear facet and a parallel line to the line connecting the posterior-most cortical surfaces of the femoral condyles.

ability. All analyses were performed in Stata 15.0 (StataCorp, College Station, TX).

Results

Patients' characteristics

Firstly we evaluated the records of 2000 knee MRIs. Overall, 400 patients were eligible to enter the study, while after applying inclusion and exclusion criteria and clinical examination, 100 cases of chondromalacia were eligible for the final analysis. We evaluated MRI findings of 200 participants, including 100 cases (50 male) with chondromalacia aged between 21 to 64, and 100 healthy controls (51

TABLE 1. MRI measurements of the control patients versus chondromalacia cases

MRI Measurements	Median (IQR)		Odds ratio	95% CI†	P-value
	Control	Case			
INA (degree)	52.0 (48.0–57.0)	53.0 (48.0–56.0)	1.00	0.96–1.05	0.863
IW (mm)	21.5 (20.1–23.4)	20.3 (19.0–21.7)	0.77	**0.67–0.88**	**< 0.001**
ID (mm)	28.2 (26.7–29.8)	25.9 (26.7–29.8)	0.76	**0.68–0.85**	**< 0.001**
MCW (mm)	26.5 (24.9–28.5)	24.8 (23.2–26.7)	0.79	**0.70–0.88**	**< 0.001**
LCW (mm)	27.2 (25.5–28.8)	24.4 (23.3–26.1)	0.77	**0.69–0.86**	**< 0.001**
ATS (degree)	8.0 (5.5–11.5)	8.0 (6.0–10.5)	1.01	0.94–1.09	0.727
CTS (degree)	3.5 (2.0–5.0)	4.0 (2.5–5.2)	1.13	0.96–1.32	0.144
MTS (degree)	7.5 (5.2–9.5)	7.0 (4.5–9.5)	0.95	0.87–1.04	0.252
LTS (degree)	5.5 (3.5–7.5)	5.5 (3.5–7.5)	0.96	0.88–1.05	0.448
PTTS angle (degree)	27.0 (23.0–30.0)	27.0 (24.0–30.0)	1.01	0.95–1.08	0.46
NWI	0.29 (0.27–0.31)	0.29 (0.27–0.31)	0.18	0.00–6399.00	0.749
TD (mm)	5.30 (4.82–5.87)	4.04 (3.51–4.60)	0.14	**0.08–0.24**	**< 0.001**
SA (degree)	140.0 (134.0–145.0)	142.0 (137.0–150.0)	1.04	**1.01–1.08**	**0.009**
LTI (degree)	20.0 (18.0–23.0)	20.0 (17.5–24.0)	0.99	0.93–1.05	0.683
MTI (degree)	18.0 (15.0–21.0)	16.0 (13.5–20)	0.93	**0.89–0.99**	**0.020**
LPTA (degree)	13.0 (10.0–16.0)	14.0 (10.5–17.0)	1.03	0.97–1.08	0.294
PFA (degree)	138.0 (133.0–142.0)	136.0 (132.5–141.0)	0.97	0.93–1.01	0.160
PFI	1.14 (1.01–1.35)	1.32 (1.07–1.59)	3.02	**1.37–6.65**	**0.006**
TTTG (mm)	12.5 (10.2–15.2)	12.3 (10.5–16.1)	1.01	0.95–1.09	0.603
SCF (mm)	20.5 (17.3–25.3)	26.7 (21.7–34.8)	1.14	**1.09–1.19**	**< 0.001**
CWI	0.52 (0.50–0.54)	0.52 (0.50–0.54)	0.76	0.00–3481.00	0.949
SWI	0.57 (0.54–0.59)	0.56 (0.54–0.58)	0.01	0.00–34.80	0.270
P-PT angle (degree)	140.5 (137.0–144.0)	140.0 (137.5–143.5)	0.99	0.93–1.05	0.802
ISI	0.98 (0.89–1.07)	1.00 (0.89–1.14)	4.62	0.60–35.20	0.139
PTI	0.31 (0.26–0.36)	0.30 (0.25–0.35)	0.04	0.00–2.21	0.115

† IQR represents 25th–75th interquartile range, 95% CI represents 95% confidence interval for odds ratio

ATS = Anterior tibial slope; CTS = Coronal tibial slope; CWI = Cartilaginous Wiberg index; ID = Intercondylar depth; INA = Intercondylar notch angle; ISI = Insall-Salvati index; IW = Intercondylar width; LCW = Lateral condyle width; LPTA = Lateral patellar tilt angle; LTI = Lateral trochlear inclination; LTS = Lateral tibial slope; MCW = Medial condyle width; MTI = Medial trochlear inclination; MTS = Medial tibial slope; NWI = Notch width index; P-PT angle = Patella-patellar tendon angle; PTTS angle = Patellar tibial tendon shaft angle; PFA = Patellar facet angle; PFI = Patellofemoral index; PTI = Patellotrochlear index; SA = Sulcus angle; SCF = Subcutaneous fat pad; SWI = Subchondral Wiberg index; TD = Trochlear depth; TTTG = Tibial tuberosity trochlear groove distance

male) aged between 20 and 57. The mean age of the chondromalacia subjects and cases were 32.7 ± 9.3 and 30.2 ± 7.2, respectively (P-value = 0.21)

Radiographic measurements

We measured 25 radiographic parameters. Table 1 summarizes the radiographic features in patients and controls. Intercondylar width, intercondylar depth, medial condyle width, lateral condyle width, trochlear depth, and medial trochlear inclination pad were significantly lower in chondromalacia cases (P-value = < 0.001, < 0.001, 0.020), while sulcus angle, patellofemoral index, and subcutaneous fat were significantly higher in cases compared to controls (P-value = 0.009, 0.006, < 0.001).

Predictive model for chondromalacia

We developed a predictive model for chondromalacia. This model included medial tibial slope, trochlear depth, lateral trochlear inclination, and lateral patellar tilt angle and age. This model predicted the disease with an excellent AUC (area under curve) of 0.92 (95% CI: 0.85–0.94). Any increase in lateral trochlear inclination and lateral patellar

TABLE 2. Predictive model for chondromalacia including MRI measurements

MRI measurements	Odds ratio	95% CI	P-value	Intra-rater reliability	Contribution of any increase in this parameter to chondromalacia
LTI	1.15	1.03–1.30	0.014	0.992	Increases disease probability
LPTA	1.13	1.02–1.26	0.018	0.996	Increases disease probability
MTS	0.85	0.73–0.98	0.026	0.997	Decreases disease probability
TD	0.06	0.02–0.17	0.000	0.995	Decreases disease probability
Age	1.10	1.02–1.20	0.015	-	Increases disease probability

LTI = Lateral trochlear inclination; LPTA = Lateral patellar tilt angle; MTS = Medial tibial slope; TD = Trochlear depth

The Area under curve (AUC) for this model is estimated as 0.92 (bootstrap bias-corrected 95% CI: 0.85–0.94). Any increase in lateral trochlear inclination and lateral patellar tilt angle could increase the probability of the disease (positive correlation), while any increase in medial tibial slope and trochlear depth could decrease the probability of the disease (negative correlation)

TABLE 3. Predictive model for chondromalacia severity including MRI measurements

MRI measurements	Odds ratio	95%CI	P-value	Intra-rater reliability	Contribution of any increase in this parameter to chondromalacia severity
ISI	75.89	2.17–2652.69	0.017	0.997	Increases disease grade
Age	1.14	1.07–1.21	0.000	-	Increase disease grade

ISI = Insall-Salvati index

The Area under curve (AUC) for this model is estimated as 0.82 (bootstrap bias-corrected 95% CI: 0.64–0.86). Grade 1 and 2 are considered as non-severe, while grade 3 and 4 are assumed as severe. Increase in patellar height and age will increase disease grade (positive correlation with disease severity)

tilt angle could increase the probability of the disease (positive correlation with chondromalacia) (Odds ratio 1.15, 1.13; 95% CI: 1.03–1.30; 1.02–1.26, respectively).

However, any increase in medial tibial slope and trochlear depth could decrease the probability of chondromalacia (negative correlation with chondromalacia) (Odds ratio 0.85, 0.06; 95% CI: 0.73–0.98, 0.02–0.17, respectively), (Table 2). Increasing age could also increase the probability of the disease (positive correlation with chondromalacia) (Odds ratio 1.10; 95%CI: 1.02–1.20).

INA, IW, ID, MCW, LCW, ATS, CTS, LTS, PTTS angle, NWI, SA, MTI, PFA, PFI, TTTG, SCF, CWI, SWI, P-PT angle, PTI, and ISI were not significant (no correlation with chondromalacia) in the multivariable analysis regarding the presence of chondromalacia (P-value = 0.20, 0.24, 0.15, 0.19, 0.56, 0.30, 0.09, 0.39, 0.43, 0.32, 0.21, 0.55, 0.07, 0.15, 0.11, 0.11, 0.19, 0.66, 0.09, 0.27, 0.29; respectively).

Predictive model for the severity of the disease

Patients were classified as grade 1 lesion (38 patients), grade 2 lesion (28 patients), grade 3 lesion (14 patients), and grade 4 lesion (20 patients). We combined grade 1 and 2 *vs.* grade 3 and 4 to develop a predictive model for severity of disease in patients with chondromalacia.

We designed a two-variable model for predicting the severity of the disease using age and Insall-Salvati index concurrently. Insall-Salvati index and age were two factors that could predict disease severity (Odds ratio = 75.89, 1.14; 95% CI: 2.17–2652.69, 1.07–1.21, respectively) with an AUC of 0.82 (95% CI: 0.64–0.86) (Table 3). Any increase in Insall-Salvati index (*i.e.* any increase in patellar height) and age could increase the severity of the disease (resulted in higher grades of chondromalacia). It means that if patellar height increases, patients will experience more severe disease (higher grades).

Discussion

Prediction models are becoming more popular in medicine. Previous studies focused their attention on the correlation between trochlear morphology and chondromalacia patellae, in a single variable analysis model. We developed a model to predict chondromalacia. We included medial tibial slope, lateral trochlear inclination, lateral patellar tilt an-

gle, trochlear depth, and age in the final predictive model for chondromalacia. We found that any increase in lateral trochlear inclination and lateral patellar tilt angle could increase the probability of the disease, while any increase in medial tibial slope and trochlear depth could decrease the probability of the disease. We also found that if patellar height increases, patients would experience more severe disease (higher grades).

Lateral patellar tilt angle (LPTA) was suggested as one of the predictive factors in the final model. LPTA was shown to be increased in chondromalacia subjects. Abnormal position of the patella in the femoral trochlear groove may play a role in the progression of chondromalacia patellae.[21,22] Studies have shown that lateral patellar displacement is associated with cartilage loss.[23] This can be justified by the fact that lateral tilting happens as a result of lateral compressive forces which acts on the lateral facet and increases shear forces in the central ridge area. These forces will increase chondrocyte activity, until the functional requests exceed chondrocyte potential and results in chondrocyte degeneration.[24] Moreover, previous studies have found that LPTA correlates with the sulcus angle in different knee flexion angles.[25] Sulcus angle has been reported to be greater in lateral maltrackers compared to non-lateral maltrackers[26], and it also correlates with cartilage lesions.[27] A wider sulcus is responsible for the increased pressure on patellofemoral articular surface and will predispose the patient to cartilage loss.[27] This correlation between the sulcus angle and LPTA may justify our result. However, LPTA has been reported to correlate significantly with chondral lesions in the lateral compartment of the patellofemoral joint (odds ratio < 1) and non-significantly with chondral lesions in the medial compartment of the patellofemoral joint (odds ratio > 1) in previous studies.[27] In this study, we did not define the side of cartilage defect. As chondromalacia impacts the medial side more frequently[28], we may speculate that this relationship in our study should be judged according to the side of involvement.

In addition, LTI was positively correlated with chondromalacia according to our results. Kuroda *et al.* showed that elevation of lateral trochlea facet (increased LTI) could increase average patellofemoral contact pressure (40% increased with 10 mm lateral trochlear elevation). This may also induce the degradation of the cartilage.[29]

The most important finding of the present study is that the tibial slope may play an important role in the progression of chondromalacia. We found that with the medial tibial slope increasing, the risk of chondromalacia decreases. Studies suggest that an increase in the tibial slope leads to a decrease in patellofemoral contact force.[30] Posterior positioning of femoral components and increase in quadriceps lever arm are responsible for this association.[31-33] We deduce that the tibial slope correlates with chondromalacia patellae; however, the effect of tibial slope on medial and lateral patellar facets may be different. Furthermore, correcting the tibial slope with a greater angle has been shown to reduce anterior tibial strains, which are imposed on the patella.[34] Moreover, studies in patients with osteoarthritis suggested that increasing the tibial slope in unicompartmental knee arthroplasty of medial patellar facet will reduce the tension on the medial side.[11] This may also show the clinical importance of tibial slope on decreasing patellofemoral stress.

Our study suggests that trochlear depth would be sufficient for measuring the association of trochlear dysplasia with chondromalacia. Sulcus angle and trochlear depth are the two important factors associated with trochlear dysplasia in previous studies[35], and the congruency of the patella and femoral trochlea has been underscored in the development of cartilage lesions.[10] Patellofemoral tracking is also considered an important factor in patellofemoral pain syndrome.[36] Trochlear depth has been reported to be an important determinant of patellofemoral stability[37], thus, it may be an important factor in the process of tracking. Tuna *et al.* reported sulcus angle and trochlear depth to be significantly different in patients with and without the disease.[18] They reported greater mean of sulcus angle and lower mean of trochlear depth in chondromalacia subjects. Our findings are consistent with the latter study. We found that with the trochlear depth decreasing, the risk of chondromalacia increases to a great extent. This may be explained by the fact that when the trochlear surface becomes shallower, the surface area for articulation at the patellofemoral joint increases. Although it may provide a better distribution of joint load[37], the increased friction may result in cartilage defects. Further studies are needed to evaluate this proposed kinematics in active knee movements. This finding may underscore the clinical importance of trochlear depth. Takahashi *et al.* also showed better adaptation of the implants featuring deep trochlea to the native patella (low-contact stress implant and NexGen implant).[38]

We also proposed a predictive model of disease severity. In our study, ISI and age could predict

higher disease severity. To our knowledge, this is the first predictive model for the severity of chondromalacia with an excellent AUC. A model was proposed in the previous study by Lu *et al*. for chondromalacia but not severity by using Insall-Salvati index (ISI). This model was based on the patella alta and baja and could diagnose chondromalacia with an AUC of 0.596.[7]

In both predictive models proposed by our findings, age was remained as an important factor. A study in the United States population showed that the contribution of chondromalacia to the patellofemoral pain syndrome increases by age up to 59 years.[39] We also excluded patients older than 65 years and the results may not be applicable to older age groups.

There are some limitations to our study. This was a single center study, we used MRI to detect chondral lesion and early lesions might be considered as normal. MRI evaluations were performed during rest. Muscle contractions may alter these findings as described by previous studies.[42] We did not evaluate the exact site of the cartilage lesions. Moreover, medial and lateral facet chondromalacia might have different natures. Previous studies reported the predominance of chondromalacia in the medial patellar facet.[22] We did not define the side of chondromalacia in our subjects, so more pieces of evidence are needed to define the exact correlation of tibial slope with both medial- and lateral-facet chondromalacia.

The advantage of this study in knowledge is that when more diverse anatomical factors are analyzed regarding the presence of chondromalacia, tibial anatomical factors play a role in the progression of the disease. This study may clarify the mechanism of chondromalacia and emphasize the role of tibial slopes in the mechanism of cartilage loss. Previous studies focused on femoral trochlear dysplasia, and did not include tibial anatomical parameters in their analysis. The result of this study meight also affect the treatment of chondromalacia, as new treatment plans for healing cartilage and bone defects are being introduced and focus on altering tibial anatomy including tubercle osteotomy.[40,41] The result of this study shew the role of tibial anatomy in developing chondromalacia. In addition, the clinical importance of this study was the fact that tibial slope should be precisely set in knee surgeries; however, more studies are needed to determine the best cut-off for tibial slope.

References

1. Endo Y, Stein BE, Potter HG. Radiologic assessment of patellofemoral pain in the athlete. *Sports Health* 2011; **3:** 195-210. doi: 10.1177/1941738110397875
2. Crossley KM, Stefanik JJ, Selfe J, Collins NJ, Davis IS, Powers CM, et al. Patellofemoral pain consensus statement from the 4th International Patellofemoral Pain Research Retreat, Manchester. Part 1: Terminology, definitions, clinical examination, natural history, patellofemoral osteoarthritis and patient-reported outcome measures. *Br J Sports Med* 2016; **50:** 839-43. doi: 10.1136/bjsports-2016-096384
3. Davies AP, Costa ML, Shepstone L, Glasgow MM, Donell S. The sulcus angle and malalignment of the extensor mechanism of the knee. *J Bone Joint Surg Br* 2000; **82:** 1162-6. doi: 10.1302/0301-620x.82b8.10833
4. Aysin IK, Askin A, Mete BD, Guvendi E, Aysin M, Kocyigit H. Investigation of the relationship between anterior knee pain and chondromalacia patellae and patellofemoral malalignment. *Eurasian J Med* 2018; **50:** 28-33. doi: 10.5152/eurasianjmed.2018.17277
5. LLopis E, Padron M. Anterior knee pain. *Eur J Radiol* 2007; **62:** 27-43. doi: 10.1016/j.ejrad.2007.01.015
6. Neusel E, Graf J. The influence of subchondral vascularisation on chondromalacia patellae. *Arch Orthop Trauma Surg* 1996; **115:** 313-5. doi: 10.1007/bf00420322
7. Lu W, Yang J, Chen S, Zhu Y, Zhu C. Abnormal patella height based on insall-salvati ratio and its correlation with patellar cartilage lesions: an extremity-dedicated low-field magnetic resonance imaging analysis of 1703 Chinese cases. *Scand J Surg* 2016; **105:** 197-203. doi: 10.1177/1457496915607409
8. Liao TC, Yin L, Powers CM. The influence of isolated femur and tibia rotations on patella cartilage stress: a sensitivity analysis. *Clin Biomech* 2018; **54:** 125-31. doi: 10.1016/j.clinbiomech.2018.03.003
9. Kok HK, Donnellan J, Ryan D, Torreggiani WC. Correlation between subcutaneous knee fat thickness and chondromalacia patellae on magnetic resonance imaging of the knee. *Can Assoc Radiol J* 2013; **64:** 182-6. doi: 10.1016/j.carj.2012.04.003
10. Ali SA, Helmer R, Terk MR. Analysis of the patellofemoral region on MRI: association of abnormal trochlear morphology with severe cartilage defects. *AJR Am J Roentgenol* 2010; **194:** 721-7. doi: 10.2214/AJR.09.3008
11. Weber P, Woiczinski M, Steinbruck A, Schmidutz F, Niethammer T, Schroder C, et al. Increase in the tibial slope in unicondylar knee replacement: analysis of the effect on the kinematics and ligaments in a weight-bearing finite element model. *Biomed Res Int* 2018; **2018:** 8743604. doi: 10.1155/2018/8743604
12. Hayes CW, Conway WF. Evaluation of articular cartilage: radiographic and cross-sectional imaging techniques. *Radiographics* 1992; **12:** 409-28. doi: 10.1148/radiographics.12.3.1609135
13. Huang M, Li Y, Guo N, Liao C, Yu B. Relationship between intercondylar notch angle and anterior cruciate ligament injury: a magnetic resonance imaging analysis. *J Int Med Res* 2019; **47:** 1602-9. doi: 10.1177/0300060518824447
14. Alentorn-Geli E, Pelfort X, Mingo F, Lizano-Diez X, Leal-Blanquet J, Torres-Claramunt R, et al. An evaluation of the association between radiographic intercondylar notch narrowing and anterior cruciate ligament injury in men: the notch angle is a better parameter than notch width. *Arthroscopy* 2015; **31:** 2004-13. doi: 10.1016/j.arthro.2015.04.088
15. K S, Chamala T, Kumar A. Comparison of anatomical risk factors for noncontact anterior cruciate ligament injury using magnetic resonance imaging. *J Clin Orthop Trauma* 2019; **10:** 143-8. doi: 10.1016/j.jcot.2017.08.002
16. Fucentese SF, von Roll A, Koch PP, Epari DR, Fuchs B, Schottle PB. The patella morphology in trochlear dysplasia--a comparative MRI study. *Knee* 2006; **13:** 145-50. doi: 10.1016/j.knee.2005.12.005
17. Aksahin E, Aktekin CN, Kocadal O, Duran S, Gunay C, Kaya D, et al. Sagittal plane tilting deformity of the patellofemoral joint: a new concept in patients with chondromalacia patella. *Knee Surg Sports Traumatol Arthrosc* 2017; **25:** 3038-45. doi: 10.1007/s00167-016-4083-4
18. Tuna BK, Semiz-Oysu A, Pekar B, Bukte Y, Hayirlioglu A. The association of patellofemoral joint morphology with chondromalacia patella: a quantitative MRI analysis. *Clin Imaging* 2014; **38:** 495-8. doi: 10.1016/j.clinimag.2014.01.012

19. Tahmasebi MN, Aghaghazvini L, Mirkarimi SS, Zehtab MJ, Sheidaie Z, Sharafatvaziri A. The influence of tibial tuberosity-trochlear groove distance on development of patellofemoral pain syndrome. *Arch Bone Jt Surg* 2019; **7:** 46-51.

20. Ozel D. The relationship between early-onset chondromalacia and the position of the patella. *Acta Radiol* 2020; **61:** 370-5. doi: 10.1177/0284185119861901

21. Hunter DJ, Zhang YQ, Niu JB, Felson DT, Kwoh K, Newman A, et al. Patella malalignment, pain and patellofemoral progression: the Health ABC Study. *Osteoarthritis Cartilage* 2007; **15:** 1120-7. doi: 10.1016/j.joca.2007.03.020

22. Fulkerson JP. *Disorders of the patellofemoral joint*. Fourth edition. Baltimor: Lippincott Williams & Wilkins; 2004.

23. Yang B, Tan H, Yang L, Dai G, Guo B. Correlating anatomy and congruence of the patellofemoral joint with cartilage lesions. *Orthopedics* 2009; **32:** 20. doi: 10.3928/01477447-20090101-27

24. Mazzola C, Mantovani D. Patellofemoral malalignment and chondral damage: current concepts. *Joints* 2013; **1:** 27-33. PMID: 25606514

25. Hoshmand LT, Helmes E, Kazarian S, Tekatch G. Evaluation of two relaxation training programs under medication and no-medication conditions. *J Clin Psychol* 1985; **41:** 22-9. doi: 10.1002/1097-4679(198501)41:1<22::aid-jclp2270410105>3.0.co;2-e

26. Harbaugh CM, Wilson NA, Sheehan FT. Correlating femoral shape with patellar kinematics in patients with patellofemoral pain. *J Orthop Res* 2010; **28:** 865-72. doi: 10.1002/jor.21101.

27. Kalichman L, Zhang Y, Niu J, Goggins J, Gale D, Felson DT, et al. The association between patellar alignment and patellofemoral joint osteoarthritis features--an MRI study. *Rheumatology* 2007; **46:** 1303-8. doi: 10.1093/rheumatology/kem095

28. Fulkerson JP, Buuck DA. *Disorders of the patellofemoral joint*. Philadelphia: Lippincott Williams & Wilkins; 2004.

29. Batailler C, Neyret P. Trochlear dysplasia: imaging and treatment options. *EFORT Open Rev* 2018; **3:** 240-7. doi: 10.1302/2058-5241.3.170058

30. Okamoto S, Mizu-uchi H, Okazaki K, Hamai S, Nakahara H, Iwamoto Y. Effect of tibial posterior slope on knee kinematics, quadriceps force, and patellofemoral contact force after posterior-stabilized total knee arthroplasty. *J Arthroplasty* 2015; **30:** 1439-43. doi: 10.1016/j.arth.2015.02.042

31. Ostermeier S, Hurschler C, Windhagen H, Stukenborg-Colsman C. In vitro investigation of the influence of tibial slope on quadriceps extension force after total knee arthroplasty. *Knee Surg Sports Traumatol Arthrosc* 2006; **14:** 934-9. doi: 10.1007/s00167-006-0078-x

32. Wachowski MM, Walde TA, Balcarek P, Schuttrumpf JP, Frosch S, Stauffenberg C, et al. Total knee replacement with natural rollback. *Ann Anat* 2012; **194:** 195-9. doi: 10.1016/j.aanat.2011.01.013

33. Browne C, Hermida JC, Bergula A, Colwell CW, Jr., D'Lima DD. Patellofemoral forces after total knee arthroplasty: effect of extensor moment arm. *Knee* 2005; **12:** 81-8. doi: 10.1016/j.knee.2004.05.006

34. Bai B, Baez J, Testa N, Kummer FJ. Effect of posterior cut angle on tibial component loading. *J Arthroplasty* 2000; **15:** 916-20. doi: 10.1054/arth.2000.9058

35. Pennock AT, Chang A, Doan J, Bomar JD, Edmonds EW. 3D knee trochlear morphology assessment by magnetic resonance imaging in patients with normal and dysplastic trochleae. *J Pediatr Orthop* 2020; **40:** 114-9. doi: 10.1097/BPO.0000000000001188

36. Powers CM. Patellar kinematics, part II: the influence of the depth of the trochlear groove in subjects with and without patellofemoral pain. *Phys Ther* 2000; **80:** 965-78. PMID: 11002432

37. Teichtahl AJ, Parkins K, Hanna F, Wluka AE, Urquhart DM, English DR, et al. The relationship between the angle of the trochlear groove and patella cartilage and bone morphology--a cross-sectional study of healthy adults. *Osteoarthritis Cartilage* 2007; **15:** 1158-62. doi: 10.1016/j.joca.2007.03.010

38. Takahashi A, Sano H, Ohnuma M, Kashiwaba M, Chiba D, Kamimura M, et al. Patellar morphology and femoral component geometry influence patellofemoral contact stress in total knee arthroplasty without patellar resurfacing. *Knee Surg Sports Traumatol Arthrosc* 2012; **20:** 1787-95. doi: 10.1007/s00167-011-1768-6

39. Glaviano NR, Kew M, Hart JM, Saliba S. Demographic and epidemiological trends in patellofemoral pain. *Int J Sports Phys Ther* 2015; **10:** 281-90. PMID: 26075143

40. Safikhani MM, Zamanian A, Ghorbani F, Asefnejad A, Shahrezaee M. Bi-layered electrospun nanofibrous polyurethane-gelatin scaffold with targeted heparin release profiles for tissue engineering applications. *J Polym Eng* 2017; **37:** 933-41. doi: 10.1515/polyeng-2016-0291

41. Jack C, Rajaratnam S, Khan H, Keast-Butler O, Butler-Manuel P, Heatley F. The modified tibial tubercle osteotomy for anterior knee pain due to chondromalacia patellae in adults: A five-year prospective study. *Bone Joint Res* 2012; **1:** 167-73. doi: 10.1302/2046-3758.18.2000083.

42. Felicio LR, Saad MC, Liporaci RF, Baffa Ado P, Dos Santos AC, Bevilaqua-Grossi D. Evaluating patellar kinematics through magnetic resonance imaging during open- and closed-kinetic-chain exercises. *J Sport Rehabil* 2010; **19:** 1-11. doi: 10.1123/jsr.19.1.1